ELSEVIER

Ceramics International 25 (1999) 375–382

CERAMICS INTERNATIONAL

Preparation and characterization of lanthanum nickel oxides by combined coprecipitation and molten salt reactions

Chen-Feng Kao*, Charng-Lih Jeng

Department of Chemical Engineering, National Cheng Kung University, Tainan, 70101, Taiwan

Received 6 March 1998; accepted 4 May 1998

Abstract

This study deals with the preparation of the lanthanum nickel oxides by combined precipitation and molten salt reactions. The reagents such as $LaCl_3$, $NiCl_2$ and different alkali metal hydroxides were used to get the precursors in various compositions. They were reacted at 1073–1173 K to obtain the fine lanthanum nickel oxides (La_2NiO_4, $LaNiO_3$) with a uniform particle size about 0.1 μm. $LaNiO_3$ is unstable at high temperature and converted into La_2NiO_4. The powders coprecipitated with potassium hydroxide have good sinterability leading to less in electrical resistivity than those with sodium hydroxide or lithium hydroxide. These compounds with different compositions exhibit characteristics of Pauli paramagnetic materials. In correspondence with the change of phase ratios there are also changes in the mass susceptibility from 4.0×10^{-6} emu/(g-Gauss) for $LaNiO_3$ to 1.25×10^{-6} emu/(g-Gauss) for La_2NiO_4.

Keywords: La_2NiO_4; $LaNiO_3$; Electrical resistivity; Magnetic susceptibility; Coprecipitation; Molten salt reactions

1. Introduction

$LaNiO_3$ is a rhombohedrally distorted perovskite-type structure. It has attracted much attention in the past few years, as a conducting layer for application in ferroelectric memories.

$LaNiO_3$ is a semiconductor material in the electrode for high temperature fuel cells [1], as a catalyst [2,3], and as a sensor for ethanol [4,5]. Its thermal stability is not so high (1170 K) [6] and it is proven to be the perovskite structure [7,8]. It contains Pauli paramagnetic and metallic behaviour. Part of Ni^{3+} is reduced to Ni^{2+} due to the influence of oxygen partial pressure during heating. Therefore, $LaNiO_3$ is converted to La_2NiO_4, as a two-dimensional structure of K_2NiF_4. In the past, the Skull melting process [9,10] was usually used. However, better chemical reactions such as coprecipitation of oxalate [11], hydroxide, cyanide and nitrate solid solution precursors [12] followed by calcination yield homogeneous oxides which exhibit good electrical [13,14] and magnetic [15–17] properties.

In this study, we have investigated the electrical and magnetic properties of the lanthanum nickel oxides (La_2NiO_4, $LaNiO_3$). There is not seen the study for the preparation of the lanthanum nickel oxides by combined coprecipitation and molten salt reactions until now. Using this above method one can obtain the lanthanum nickel oxide in lower temperature and produce uniform ceramic powders. Therefore, this method is more efficient and more popular to the application of materials.

We also investigate the system further, and analyze the effect of homogeneity, particle size distribution, calcining temperature and formation of phase from the precursors derived by chemical coprecipitation. Finally, from the sintered bodies we can study the sinterability, electrical and magnetic properties in order to test its suitability as an electronic ceramic.

Kao et al. have studied the preparation and characterization of fine La–Cr–Zr oxide ceramics by chemical coprecipitation at high temperature [18].

2. Theory

Coprecipitation combined with high temperature melting [19] was used to form lanthanum nickel oxides. The advantage of this method is that salts, such as NaCl, LiCl or KCl that are formed as by products

* Corresponding author.

0272-8842/99/$20.00
PII: S0272-8842(98)00047-9

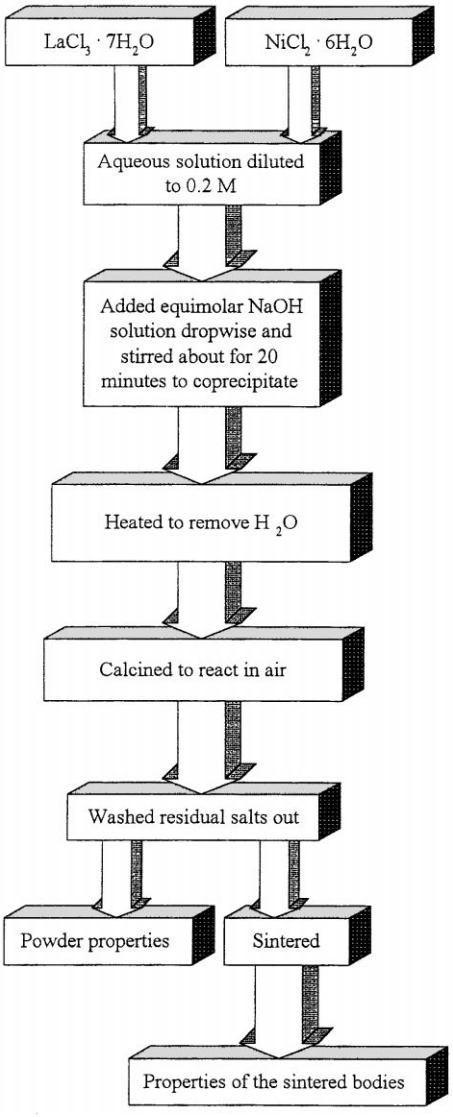

Fig. 1. The flow chart for combining precipitation and molten salt reactions.

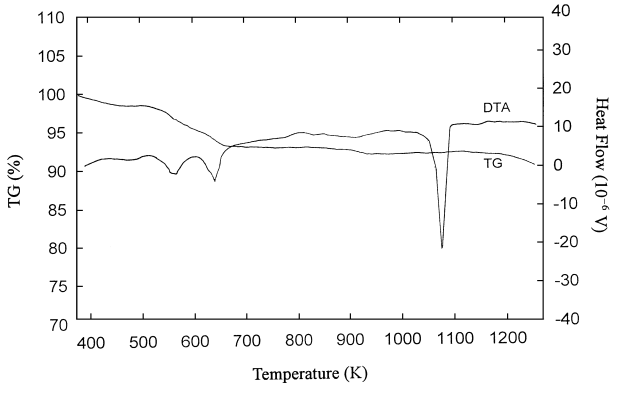

Fig. 2. The results of the thermogravity analysis and differential thermal analysis of the precursor.

during co-precipitation were not washed out. They act as a flux in which the precipitates dissolve and react to give oxides. The salt is then washed out with distilled water after calcining procedure and the fine particles of pure oxides were obtained and were easily sintered. This process control is much easier than any other, and the dissolved salt is as an auxiliary agent in reaction. The oxides from this method have more uniform and much better particle size distribution than those of solid-state reaction or general coprecipitation.

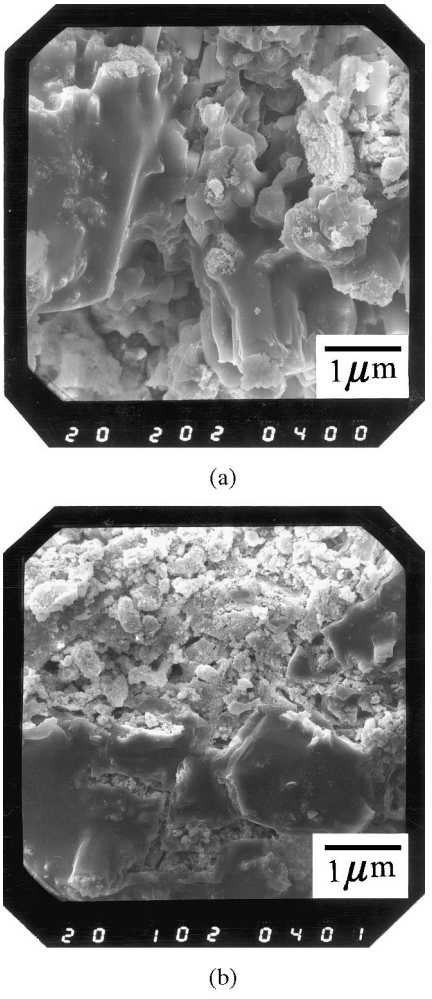

Fig. 3. The SEM images in 5 K magnification of the coprecipitated samples (a) La:Ni = 1:1 (b) La:Ni = 2:1 in NaOH.

Table 1
The shrinkage, bulk density and apparent density of sintered discs that coprecipitated with NaOH in different sintering temperature

Temperature (K)	Property		
	Shrinkage (%)	Bulk density (g/cm^3)	Apparent density (g/cm^3)
1473	6.2	4.11	4.78
1573	12.3	5.14	6.02
1673	14.5	5.64	6.17

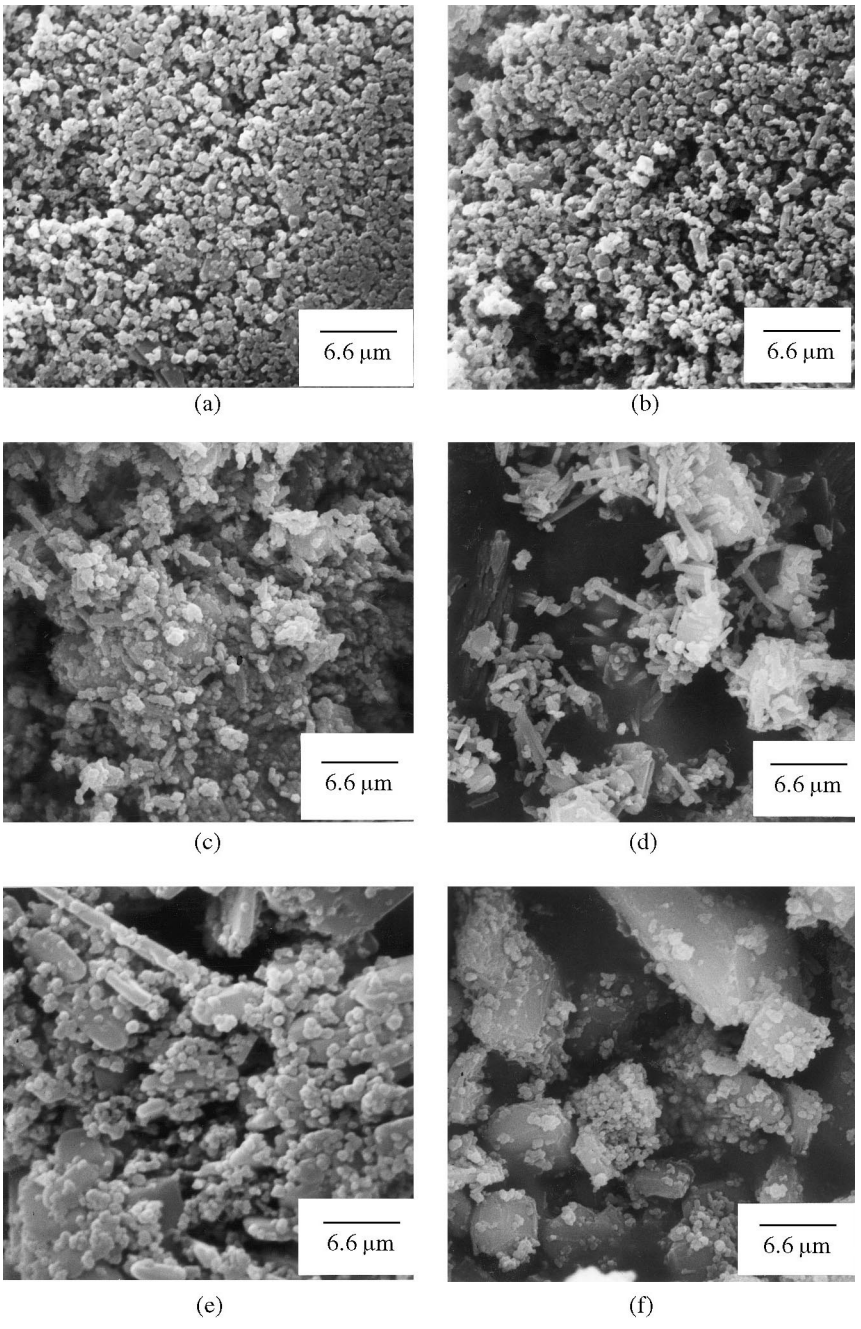

Fig. 4. The SEM images in 15 K magnification of the calcined samples: (a) La:Ni = 1:1 at 1073 K with NaCl; (b) La:Ni = 2:1 at 1073 K with NaCl; (c) La:Ni = 1:1 at 1173 K with KCl; (d) La:Ni = 2:1 at 1173 K with KCl; (e) La:Ni = 1:1 at 973 K with LiCl; (f) La:Ni = 2:1 at 973 K with LiCl.

The reactions in this study can be written as follows:

$$2LaCl_3 + NiCl_2 + 8NaCl \rightarrow 2La(OH)_3 + Ni(OH)_2 + 8NaCl \rightarrow La_2NiO_4 + 8NaCl + 4H_2O \uparrow$$

Owing to a eutectic melting of the salt one can effectively decrease the calcination temperature to reduce energy consumption. The existence and function of liquid melting salt, are to give more uniformity and enhance the reaction rate. This makes it better than the general solid-state reaction.

3. Experimental

A mixture of lanthanum chloride (5.94 g, Fisher Scientific Company, certified) and nickel chloride (3.80 g, Ferak GR.) with the ratio of La:Ni being 1:1 was dissolved in water and diluted to 0.2 M solution. There is alkali metal hydroxide solution, such as LiOH, NaOH or KOH, was used to mix with the above solution to form a lanthanum nickel hydroxide precursor. The oven drying was succeeded to obtain dry precursors with different kind of salt that corresponds to the coprecipited reagent.

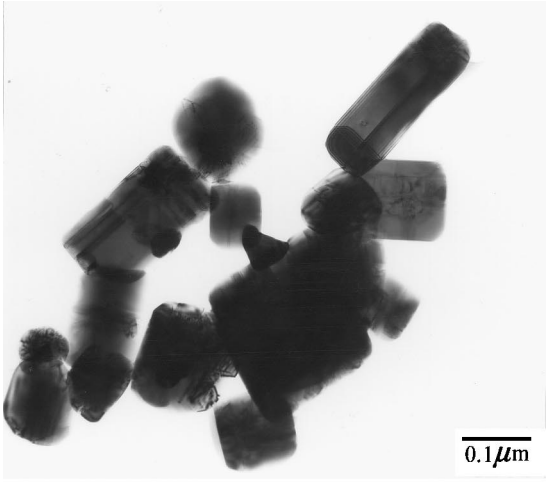

(a)

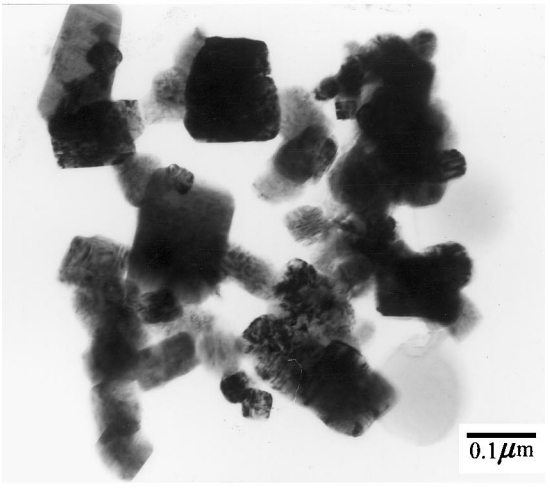

(b)

Fig. 5. The TEM images of the samples that coprecipitated with NaOH: (a) La:Ni = 1:1; (b) La:Ni = 2:1 calcined at 1073 K.

Solid-phase samples by oven drying were calcined at 973, 1073 and 1173 K, respectively. The salt was acted as a flux to improve the reactivity of precursor. The precursor washed with distilled water and filtered repeatedly to obtain fine oxide particles. The silver nitrate solution was used to prove chloride ion existent in the oxide or not.

Fig. 1 shows the flow chart for the process in this study. To analyze by a Setaram TG/DTA 92 thermogravimetric apparatus 0.04 g dry precursors were proceeded. X-ray diffractometer (XRD) with CuK_{α} radiation was used to identify the phases of oxides. A Jeol JSM-35 scanning electron microscope (SEM) was employed to study the particle morphology. Superconducting quantum interference device (SQUID Quantum Design MPMS7) magnetometer was performed magnetic measurement of the oxides in the temperature range 10–400 K [20]. The conductivities of the bulk samples of the oxides were measured with an Digital Electrometer (Advantest Co. TR-8652 type).

4. Results and discussion

4.1. Thermogravity and calcining

The typical thermogravimetric analysis (TGA) and differential thermal analysis (DTA) curves, shown in Fig. 2, are in agreement with the combined thermal behaviors of lanthanum hydroxide and nickel hydroxide. The endothermal peak at about 1073 K is melting point of sodium chloride [21–25]. So the calcining at a heating rate of 10 K/min and then the temperature was maintained at 973, 1073 or 1173 K for 8 h. These calcining temperatures also contain the range of melting points of three salts NaCl, LiCl and KCl. The precursors were calcined to become the desired oxides.

4.2. SEM analysis of the precursor (the coprecipitated powder)

The powders were dispersed in ethanol then few droplets were dipped out with a pipet into a filter paper. Cut off a small piece to be plated with gold for SEM examination. As shown in Fig. 3, the coprecipitated powders are mostly the agglomeration of small particles. This phenomenon is caused by loosing large amount of solvent from drying powders [26,27]. There is also agglomeration due to the existence of salt. Appropriate grinding, improving the drying mode or treating with other solvents can decrease the agglomeration [28]. Agglomeration is not a severe problem for the precursors to decompose into fine particle size after calcining. Salts would be at the surface of oxides and be easy to be washed out.

4.3. SEM analysis of the calcined powder

The SEM analyses of the calcined powders were shown in Fig. 4, the uniformity of these powders is better than that of the coprecipitated powders, and the degree of agglomeration of the calcined particle is less. It is obvious from TEM analyses in Fig. 5, the shape of the particle is mostly square and its particle size distribution is also more uniform, particles are crystalline and the particle size is about 0.1 μm.

4.4. The properties of the sintered bodies

4.4.1. The shrinkage, bulk density and apparent density of the sintered bodies

The shrinkage, bulk density and apparent density of the sintered bodies at various ratios increase. The bodies

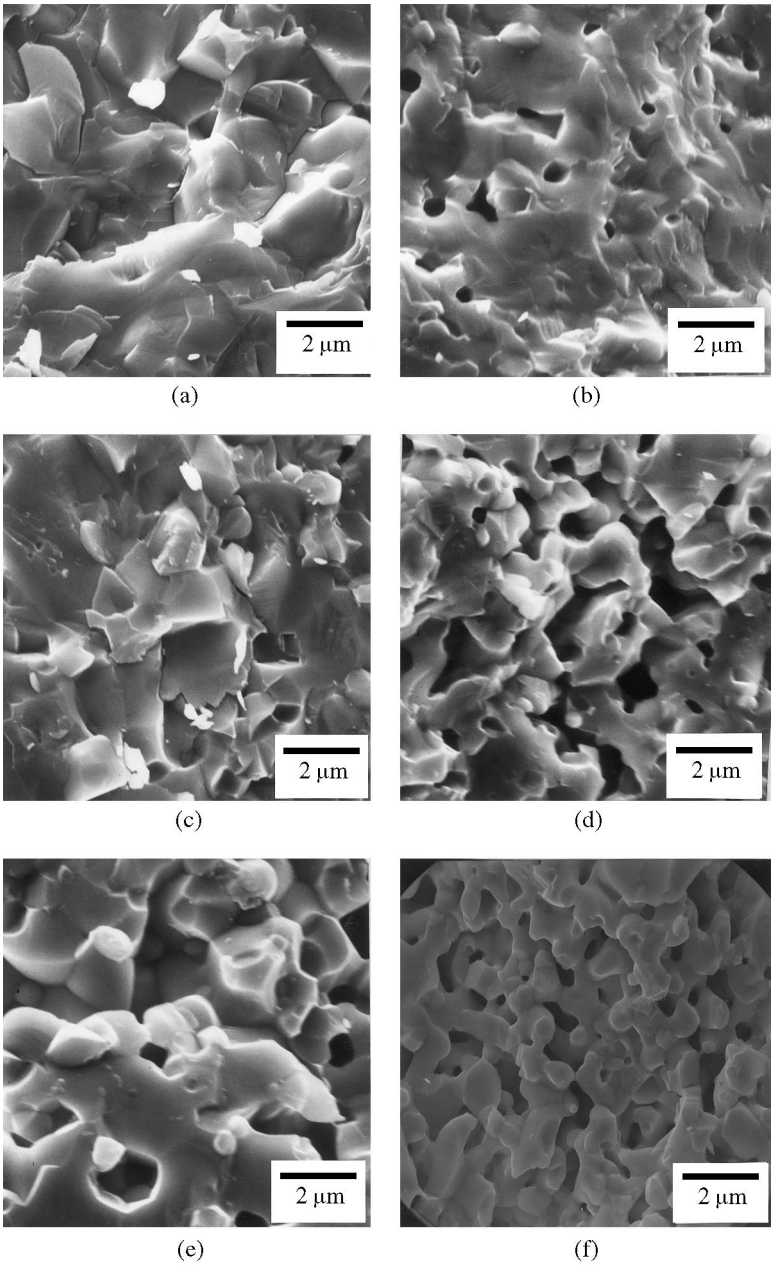

Fig. 6. The SEM images in 15 K magnification of the sintering samples: (a) La:Ni = 1:1 at 1673 K with NaCl; (b) La:Ni = 2:1 at 1573 K with NaCl; (c) La:Ni = 1:1 at 1673 K with KCl; (d) La:Ni = 2:1 at 1573 K with KCl; (e) La:Ni = 1:1 at 1673 K with LiCl; (f) La:Ni = 2:1 at 1573 K with LiCl.

become denser according to the increase in the sintering temperature as listed in Table 1. Compared with the auxiliary melting agents, the largest shrinkage is observed in KCl, the next is in NaCl and the least is in LiCl. The more the shrinkage becomes, the better the density is and the less the resistivity gives. The resistivity can be approved by electrical measurement.

4.4.2. SEM analysis of the sintered bodies

The SEM analyses of the sintered bodies at various ratios and at various sintering temperatures are shown in Fig. 6. It is indicated from Fig. 6 that sinterability becomes better as the temperature increases, in agreement with the relationship of the density of the sintered body with temperature. Compared with electrical measurement, the density and porosity of the sintered body have the relationship with its electrical property.

4.5. XRD analysis

The XRD analyses of the samples at different ratios calcined at 973, 1073 and 1173 K for 8 h are shown in Fig. 7(A) and (B). Using NaCl as a flux, the formation of $LaNiO_3$ is best at 1073 K and some is converted to

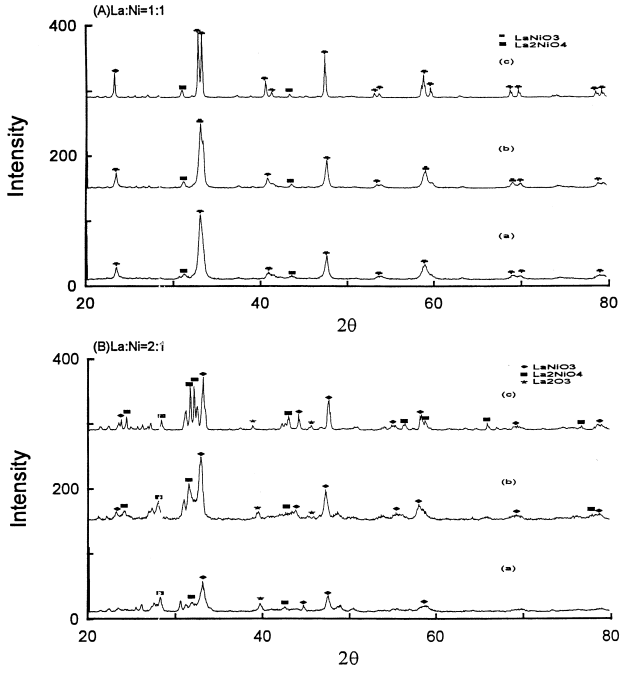

Fig. 7. The XRD patterns of the sample that (A) La:Ni = 1:1, (B) La:Ni = 2:1 with NaCl was calcined at (a) 973 K, (b) 1073 K, (c) 1173 K.

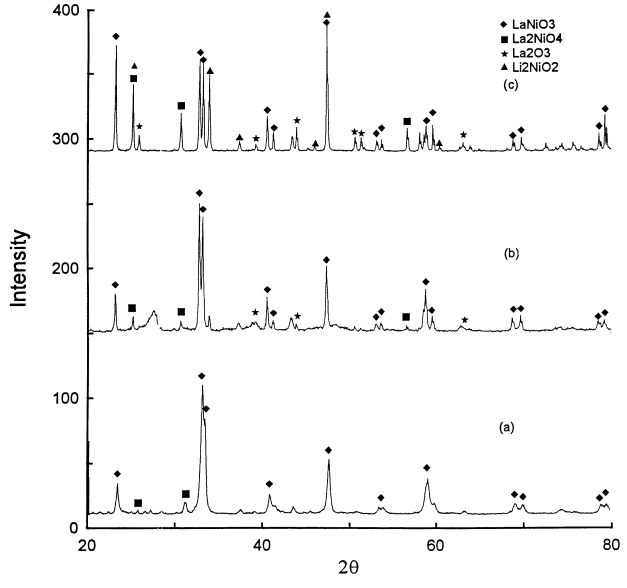

Fig. 8. The XRD patterns of the sample that La:Ni = 1:1 was coprecipitated with (a) NaOH, (b) KOH, (c) LiOH that was calcined at 1073 K.

La_2NiO_4 at 1173 K, and the unreacted La_2O_3 also appears in these compounds.

For the same purpose, the product for NaCl or KCl as auxiliary melting is the same although the reaction temperatures are different. But for LiCl the product is very different from that of NaCl or KCl, and this can be obvious from Fig. 8. The radius of Li^+ is less than that of Na^+ or K^+ (for coordination number being 6, $Li^+ = 0.74$Å, $Na^+ = 1.02$Å, $K^+ = 1.38$ Å), and gives a

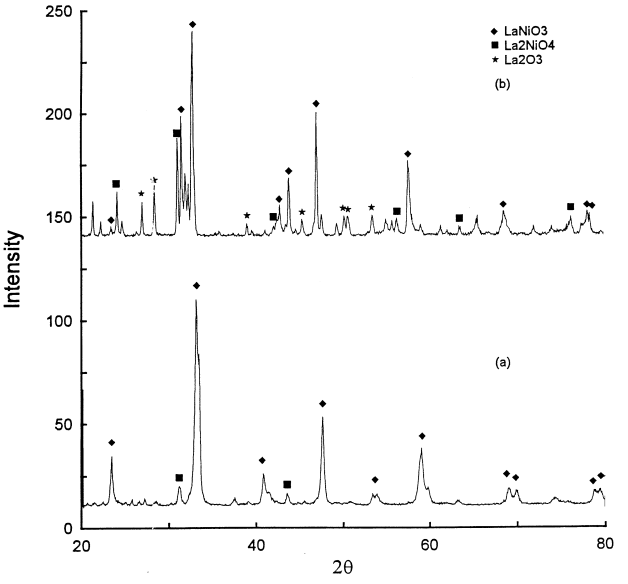

Fig. 9. The XRD patterns of the sample that La:Ni = 1:1 with NaCl was calcined at (a) 1073 K and sintered at (b) 1673 K.

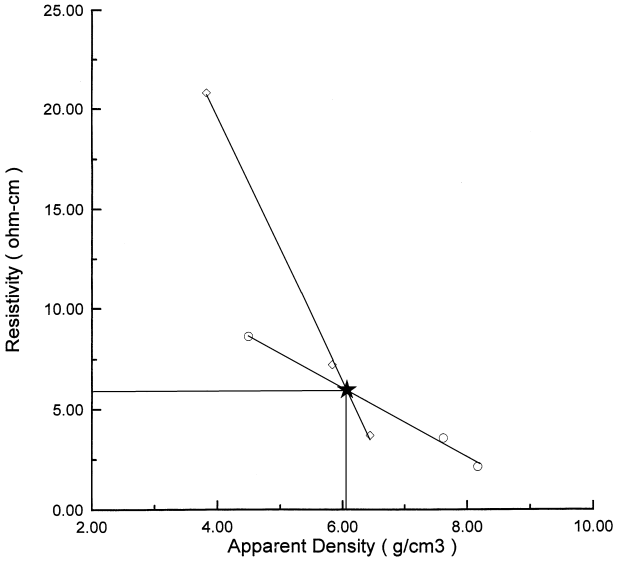

Fig. 10. The relationship of the resistivity with apparent density. (◇ $LaNiO_3$, ○ La_2NiO_4)

Li_2NiO_2. Therefore, the reaction temperature is lower for LiCl as auxiliary melting. It is discovered that there is a clear crystalline phase Li_2NiO_2 at 973 K, but it is not expected in this study.

The product after pressing under 200 MPa was sintered at 1473, 1573 or 1673 K and the density is increased and its crystal phase is more clear. Comparing the patterns of the calcined powder with those of the sintered body, it is obvious from Fig. 9 that the crystal phase of the powder after sintering is different from that of the calcined powder, indicating that it is not completely $LaNiO_3$. Comparing with that of La_2NiO_4 again, it is indicated that besides the effect of sintering at

1673 K, $LaNiO_3$ is converted into La_2NiO_4. Therefore it is clear that $LaNiO_3$ is unstable phase at high temperature, and it can be converted into La_2NiO_4 phase.

4.6. Measurement of resistivity

The resistivity of the material at various ratios has the relationship with its apparent density, or the more denser the sintered body, the better its conductivity.

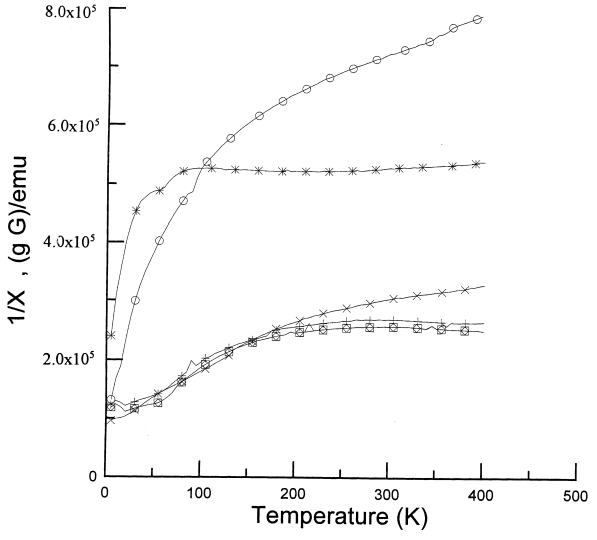

Fig. 11. The relationship of the reciprocal susceptibility with temperature for the sample that La:Ni = 1:1 was calcined at 1173 K and sintered at 1673 K. + La:Ni = 1:1, NaCl, 1173 K, ⊟ La:Ni = 1:1, KCl, 1173 K, ✕ La:Ni = 1:1, LiCl, 1173 K, ✳ La:Ni = 1:1, NaCl, 1673 K, ◇ La:Ni = 1:1, KCl, 1673 K, ○ La:Ni = 1:1, LiCl, 1673 K.

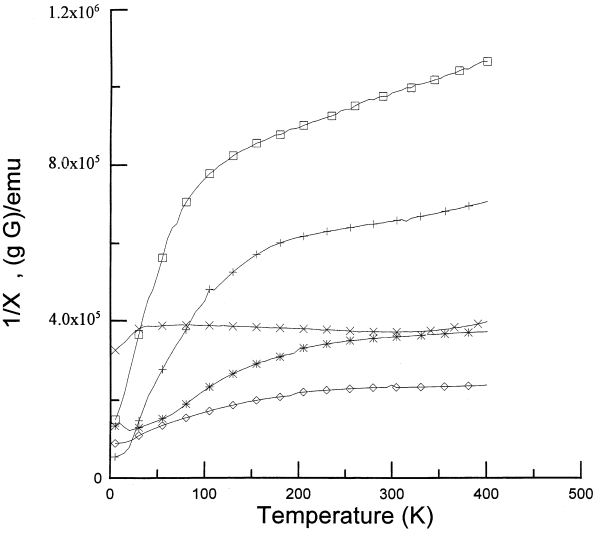

Fig. 12. The relationship of the reciprocal susceptibility with temperature for the sample that La:Ni = 2:1 was calcined at 1173 K and sintered at 1673 K. + La:Ni = 2:1, NaCl, 1173 K, ⊟ La:Ni = 2:1, KCl, 1173 K, ✕ La:Ni = 2:1, LiCl, 1173 K, ✳ La:Ni = 2:1, NaCl, 1673 K, ◇ La:Ni = 2:1, KCl, 1673 K.

It is obvious from Fig. 10 that the change in the resistivity of $LaNiO_3$ with its apparent density is larger (the slope is larger) than that of La_2NiO_4. In general, compared with the sintered body, when one wants to have lower resistivity of $LaNiO_3$, its apparent density should be over 6.0 g/cm^3 and its resistivity could be lower than 6.0 ohm-cm. But the increase in density is dependent on the increasing effect of sintering. However, only that increasing the sintering temperature, leads to decomposition of $LaNiO_3$, confirmed by XRD analysis. Therefore, the temperature has to be carefully controlled for sintering purpose.

4.7. Magnetic determination

SQUID was used to measure the reciprocal of susceptibility with temperature [20] and the results are shown in Figs. 11 and 12. It appears to be Pauli paramagnetism from the shape of the curves of Figs. 11 and 12. For La:Ni = 1:1 (Fig. 11) the susceptibility changes to appear to be low after sintering and the deviation is also larger, especially for LiCl the susceptibility at room temperature is about 1.43×10^{-6} emu/(g-Gauss). But for the other powder the susceptibility at room temperature is about 4.0×10^{-6} emu/(g-Gauss). Comparing the powder with that of the sintered body for La:Ni = 2:1 (Fig. 12), there are larger differences in the susceptibility at room temperature, but basically the value difference at 0 K is not so big.

The asymptotic Curie points and mass susceptibilities for various samples showed in Figs. 11 and 12 are summarized as Table 2.

5. Conclusions

1. The $LaNiO_3$ and La_2NiO_4 could be obtained from coprecipiting with NaOH or KOH in about 0.2–0.4 M aqueous solution, but not with LiOH.

Table 2
Asymptotic Curie point and mass susceptibility for the samples calcined with different salt and sintered in different temperature

Samples	Asymptotic Curie point (K)	Mass susceptibility $\times10^5$ [emu/g-Gauss]
La:Ni = 2:1, NaCl, 1173 K	−16.58	9.92
La:Ni = 2:1, KCl, 1173 K	−27.41	1.00
La:Ni = 2:1, LiCl, 1173 K	−137.70	0.32
La:Ni = 2:1, NaCl, 1673 K	−47.23	1.41
La:Ni = 2:1, KCl, 1673 K	−112.46	1.11
La:Ni = 1:1, NaCl, 1173 K	−77.90	1.18
La:Ni = 1:1, KCl, 1173 K	−54.06	1.54
La:Ni = 1:1, LiCl, 1173 K	−103.22	1.09
La:Ni = 1:1, NaCl, 1673 K	−30.86	0.43
La:Ni = 1:1, KCl, 1673 K	−26.73	0.64
La:Ni = 1:1, LiCl, 1673 K	−15.09	1.00

2. According to the experimental results, the $LaNiO_3$ and La_2NiO_4 could be synthesized by calcining its precursor at 1073 K for 8 h with NaCl and at 1173 K for 8 h with KCl, respectively.
3. Using NaCl as a flux, the formation of $LaNiO_3$ is best at 1073 K and some is converted to La_2NiO_4 at 1173 K.
4. The reaction temperature is lower for LiCl as auxiliary melting. It is discovered that there is a clear crystalline phase Li_2NiO_2 at 973 K, but it is not expected in this study.
5. The apparent density of sintered body of $LaNiO_3$ should be over 6.0 g/cm^3 for leading to be lower than 6.0 ohm-cm in resistivity.
6. The results of the reciprocal of susceptibility vs the temperature are found to be Pauli paramagnetism. The susceptibility variations were low after sintering and the deviations from calcined sample were larger. Especially for LiCl the susceptibility is about 1.43×10^{-6} emu/(g-Gauss) at room temperature. But for $LaNiO_3$ from KCl or NaCl the susceptibility is about 4.0×10^{-6} emu/(g-Gauss) at room temperature.

Acknowledgements

The authors thank the National Science Council, NSC 82-0402-E-006-380, for the financial support of this work.

References

[1] H.S. Spacil, C.S. Tedmon, Electrochemical behavior of the Perovskite-type $Nd_{1-x}Sr_xCoO_3$ in an aqueous alkaline solution, J. Electrochem. Soc. 122 (1975) 159.
[2] J. Drennan, C.P. Tavares, B.C.H. Steele, An electron microscope investigation of phase in the system La–Ni–O, Mat. Res. Bull. 17 (1982) 621–626.
[3] T. Kai, T. Takahashi, Kinetics of the methanation of carbon dioxide over a supported Ni–La_2O_3 catalyst, Canadian J. Chemical Engineering 66 (1988) 343–347.
[4] H. Obayashi, Y. Sakurai, T. Gejo, Perovskite-type oxide as ethanol sensors, J. Solid State Chem. 17 (1976) 299.
[5] J. Tamaki, T. Maekawa, S. Matsushima, N. Miura, N. Yamazoe, Ethanol gas sensing properties of Pd–La_2O_3–In_2O_3 thick film element, Chemistry Letters 3 (1990) 477–480.
[6] P. Odier, Y. Nigara, J. Coutures, Phase relations in the La–Ni–O system: influence of temperature and stoichiometry on the structure of La_2NiO_4, J. Solid State Chemistry 56 (1985) 32–40.
[7] P. Ganguly, C.N.R. Rao, Electron transport properties of transition metal oxide systems with the K_2NiF_4 structure, Mat. Res. Bull. 8 (1973) 405–412.
[8] T. Nakamura, G. Petzow, L.J. Gauckler, Stability of the perovskite phase $LaBO_3$ (B = V, Cr, Mn, Fe, Co, Ni) in reducing atmosphere, 1. Experimental results, Mat. Res. Bull. 14 (1979) 649–659.
[9] H.R. Harrison, R. Aragon, C.J. Sandberg, Single crystal growth of the transition metal monoxides by skull melting, Mat. Res. Bull. 15 (1980) 571–580.
[10] H.R. Harrison, R. Aragon, Skull melter growth of magnetite (Fe_3O_4), Mat. Res. Bull. 13 (1978) 1097–1104.
[11] J. Takahashi, T. Toyoda, T. Ito, M. Takatsu, Preparation of $LaNiO_3$ powder from coprecipitated lanthanum–nickel oxalates, J. Mat. Sci. 25 (1990) 1557–1562.
[12] K. Vidyasagar, J. Gopalakrishan, C.N.R. Rao, Synthesis of complex metal oxides using hydroxide, cyanide, and nitrate solid solution precursors, J. Solid State Chemistry 58 (1985) 29–37.
[13] R.A. Mohanram, L. Ganapathi, P. Ganguly, C.N.R. Rao, Further evidence for the coexistence of localized and itinerant 3d electrons in La_2NiO_4, J. Solid State Chemistry 63 (1986) 139–147.
[14] J.B. Goodenough, S. Ramasesha, Evolution of three dimensional character across the $La_{n+1}Ni_nO_{3n+1}$ homologous series with increase in n^1, Mat. Res. Bull. 17 (1982) 383–390.
[15] C.N.R. Rao, D.J. Buttrey, N. Otsuka, P. Ganguly, H.R. Sandberg, C.J. Sandberg, J.M. Honig, Crystal structure and semiconductor–metal transition of the quasi-two-dimensional transition metal oxide, La_2NiO_4, J. Solid State Chemistry 51 (1984) 266–269.
[16] B. Morten, M. Prudenziati, F. Sirotti, G. De. Cicco, A. Alberigi-Quaranta, Magnetoresistive properties of Ni-based thick films, J. Mat. Sci. in Electronics 1 (1990) 118–122.
[17] J.B. Goodenough, Interpretation of the transport properties of Ln_2NiO_4 and Ln_2CuO_4 compound, Mat. Res. Bull. 8 (1973) 423–432.
[18] Chen-Feng Kao, Jyh-Shen Jou, Preparation and characterization of fine La-Cr-Zr oxide ceramics by chemical coprecipitation at high temperatures, Ceramic Transactions (USA), 71 (1996) 521–538.
[19] Zong-Yu Zheng, Bi-Jun Guo, Xue-Ming Mei, A new technology of coprecipitation combined with high temperature melting for preparing single crystal ferrite powder, J. Magnetism and Magnetic Materials 78 (1989) 73–76.
[20] S. Chikazumi, S.H. Charap, Physics of Magnetism, John Wiley & Sons, New York, 1964, pp. 79–99 (Chapter 5).
[21] W.W.M. Wendlandt, Thermal Analysis, third ed., John Wiley & Sons, 1985, pp. 147–184.
[22] J. Sun, T. Kyotani, A. Tomita, Preparation characterization of lanthanum carbonate hydroxide, J. Solid State Chemistry 65 (1986) 94–99.
[23] S. Bernal, F.J. Botana, R. Garcia, J.M. Rodriguez Izquiedo, Thermal evolution of a sample of La_2O_3 exposed to the atmosphere, Thermochim Acta 66 (1983) 139–145.
[24] M.P. Rosynek, D.T. Magnuson, Preparation and characterization of catalytic lanthanum oxide, J. Catalysis 46 (1977) 402–413.
[25] K.R. Barnard, K. Foger, T.W. Turney, R.D. Williams, Lanthanum cobalt oxide oxidation catalysts derived from mixed hydroxide precursors, J. Catalysis 125 (1990) 265–275.
[26] D.W. Johnson Jr, P.K. Gallagher, Reactive powders from solution in ceramic processing before firing, in: G.Y. Onada Jr, L.L. Hench, (Eds.),Ceramic Processing Before Firing, John Wiley & Sons, 1978, pp. 125–139.
[27] S.L. Dole, R.W. Scheidecker, L.E. Shiers, M.F. Berard, O. Hunter Jr, Technique for preparing highly-sinterable oxide powders, Mat. Sci. and Eng. A 32 (1978) 277–281.
[28] R.E. Riman, D.M. Haaland, C.J.M. Northrup Jr, H.K. Bowen, A. Bleier, An infrared study of metal isopropoxide precursors for $SrTiO_3$, in: C.J. Brinker, D.E. Clark, D.R. Ulrich (Eds.), Better Ceramics Through Chemistry, Vol. 32, North-Holland, 1984, pp. 233–238.